



Published in final edited form as:

*N Engl J Med.* 2011 July 28; 365(4): 295–306. doi:10.1056/NEJMoa1101273.

## MYO1E MUTATIONS AND CHILDHOOD FAMILIAL FOCAL SEGMENTAL GLOMERULOSCLEROSIS

Caterina Mele, Biol.Sci.D.<sup>1,\*</sup>, Paraskevas Iatropoulos, M.D.<sup>1,\*</sup>, Roberta Donadelli, Biol.Sci.D.<sup>1</sup>, Andrea Calabria, Eng.D.<sup>2</sup>, Ramona Maranta, Biol. Sci.D.<sup>1</sup>, Paola Cassis, Ph.D.<sup>1</sup>, Simona Buelli, Ph.D.<sup>3</sup>, Susanna Tomasoni, Ph.D.<sup>3</sup>, Rossella Piras, Chem.Pharm.D.<sup>1</sup>, Mira Krendel, Ph.D.<sup>4</sup>, Serena Bettoni, Biol.Sci.D.<sup>1</sup>, Marina Morigi, Ph.D.<sup>3</sup>, Massimo Delledonne, Ph.D.<sup>5</sup>, Carmine Pecoraro, M.D.<sup>6</sup>, Isabella Abbate, Ph.D.<sup>7</sup>, Maria Rosaria Capobianchi, Ph.D.<sup>7</sup>, Friedhelm Hildebrandt, M.D.<sup>8,9</sup>, Edgar Otto, M.D.<sup>8</sup>, Franz Schaefer, M.D.<sup>10</sup>, Fabio Macchiardi, M.D.<sup>2</sup>, Fatih Ozaltin, M.D.<sup>11</sup>, Sevinc Emre, M.D.<sup>12</sup>, Tulin Ibsirlioglu, Ph.D.<sup>11</sup>, Ariela Benigni, Ph.D.<sup>3</sup>, Giuseppe Remuzzi, M.D.<sup>1,3,13,°</sup>, and Marina Noris, Ph.D.<sup>1,°</sup> on behalf of the PodoNet consortium

<sup>1</sup>Mario Negri Institute for Pharmacological Research, Clinical Research Center for Rare Diseases 'Aldo e Cele Daccò', Ranica, Bergamo, Italy

<sup>2</sup>Department of Medicine, Surgery and Dentistry, Università degli Studi di Milano, Milan, Italy

<sup>3</sup>Mario Negri Institute for Pharmacological Research, Centro Anna Maria Astori Science and Technology Park Kilometro Rosso, Bergamo, Italy

<sup>4</sup>Department of Cell and Developmental Biology, SUNY Upstate Medical University, Syracuse, NY, USA

<sup>5</sup>Center of Functional Genomics, Department of Biotechnologies, University of Verona, Verona Italy

<sup>6</sup>Department of Nephrology and Dialysis 'Santobono' Hospital, Napoli, Italy

<sup>7</sup>Laboratory of Virology, INMI L. Spallanzani, Rome, Italy

<sup>8</sup>Department of Pediatrics, University of Michigan, Ann Arbor MI, USA

<sup>9</sup>Howard Hughes Medical Institute, University of Michigan, Ann Arbor MI, USA

<sup>10</sup>Pediatric Nephrology Division, Center for Pediatrics and Adolescent Medicine, Heidelberg, Germany

<sup>11</sup>Department of Pediatric Nephrology, Hacettepe University Faculty of Medicine, Ankara, Turkey

<sup>12</sup>Department of Pediatric Nephrology, Istanbul Medical Faculty, Istanbul University, Istanbul, Turkey

<sup>13</sup>Unit of Nephrology and Dialysis, Ospedali Riuniti di Bergamo, Bergamo Italy

### Abstract

**Background**—Focal segmental glomerulosclerosis (FSGS) is a kidney disease that presents with nephrotic syndrome and is often resistant to glucocorticosteroids and progresses to end-stage

---

**Correspondence to:** Giuseppe Remuzzi, M.D., Mario Negri Institute for Pharmacological Research, Centro Anna Maria Astori, Science and Technology Park Kilometro Rosso, Via Stezzano, 87, 24126 Bergamo, Italy, Tel: 0039-035-42131, Fax: 0039-035-319331, giuseppe.remuzzi@marionegri.it.

\*These authors equally contributed to the first authorship

°These authors equally contributed to the senior authorship

kidney disease in 50–70% of patients. Genetic studies in familial FSGS indicate that it is a disease of the podocytes, major components of the glomerular filtration barrier. However the molecular cause of over half of primary FSGS is unknown, and effective treatments have been elusive.

**Methods**—We performed whole-genome linkage analysis followed by high-throughput sequencing of the positive linkage area in a family with autosomal recessive FSGS and sequenced a newly discovered gene in 52 unrelated FSGS patients. Immunohistochemistry was performed in human kidney biopsies and cultured podocytes. Expression studies *in vitro* were performed to characterize the functional consequences of the mutations identified.

**Results**—Two mutations (A159P and Y695X) in *MYO1E*, encoding the non-muscle class I myosin, myosin 1E (Myo1E), which segregated with FSGS in two independent pedigrees were identified. Patients were homozygous for the mutations and were resistant to glucocorticosteroids. Electron microscopy showed thickening and disorganization of the glomerular basement membrane. Normal expression of Myo1E was documented in control human kidney biopsies *in vivo* and in glomerular podocytes *in vitro*. Transfection studies revealed abnormal subcellular localization and function of A159P-Myo1E mutant. The Y695X mutation causes loss of calmodulin binding and the tail domains of Myo1E.

**Conclusions**—*MYO1E* mutations lead to childhood onset steroid-resistant FSGS. These data support a role of Myo1E in podocyte function and the consequent integrity of the glomerular permselectivity barrier.

---

Focal segmental glomerulosclerosis (FSGS) is a kidney lesion characterized by glomerulosclerosis that is focal, involving a subset of glomeruli, and segmental, involving a portion of the glomerular tuft. As the disease progresses, the pattern of glomerulosclerosis becomes predominantly global. Alterations of the podocytes, which develop foot-process effacement, constitute the major ultrastructural abnormality. The pathologic classification of FSGS includes collapsing, tip lesion, cellular and perihilar variants, and FSGS not otherwise specified (NOS).<sup>1</sup> FSGS may be primary, but secondary FSGS has been associated with drug toxicity, viral infections, or with diseases that affect renal mass and glomerular hemodynamics.<sup>2</sup> Genetic forms of FSGS have been reported; some affect the kidney exclusively, while others are syndromic with multi-organ involvement.<sup>3–5</sup> Genetic forms of FSGS are usually glucocorticosteroid resistant and often progress to end-stage kidney disease (ESKD).<sup>4</sup>

FSGS generally presents with proteinuria, often nephrotic range, due to dysfunction of the glomerular filtration barrier.<sup>6</sup> FSGS accounts for 7–20% of childhood nephrotic syndrome cases<sup>7</sup> and up to 35% of adult cases.<sup>8,9</sup> The incidence of FSGS appears to be increasing.<sup>7,10</sup>

An understanding of the glomerular filtration barrier is key to discussions of FSGS. It is tripartite—composed of a fenestrated endothelium, the glomerular basement membrane, and podocytes, differentiated epithelial cells with interdigitated foot processes interconnected by multi-protein slit diaphragms.<sup>6</sup> Genetic studies in familial forms indicate that FSGS is associated with mutations in genes encoding several podocyte proteins.<sup>11–18</sup> However the molecular cause of over 50% of primary, steroid-resistant FSGS is unknown, and effective treatments are lacking.<sup>3</sup>

In the present work, we used whole-genome linkage analysis and high-throughput sequencing in a family with autosomal recessive FSGS and identified a missense mutation in *MYO1E*, which encodes the non-muscle class I myosin, myosin 1E (Myo1E) and appears to cause the disease. Wild-type Myo1E is mainly expressed at the plasma membrane, but the mutant Myo1E localized to the podocyte cytoplasm. We also sequenced *MYO1E* in additional patients and identified another mutation that causes protein truncation and leads

to FSGS. Together, these findings define an important role of Myo1E for maintaining the function of the glomerular filtration barrier in humans.

## PATIENTS AND METHODS

### Study Participants

The index family (Fig. 1A) was from Italy and included three siblings with childhood-onset nephrotic syndrome and FSGS lesions on kidney biopsy and their consanguineous unaffected parents.

Additional unrelated patients with familial recessive (n=28) or sporadic childhood-onset (<13 years, n=24) FSGS, were recruited. Since mutations in the same gene may associate with either FSGS or diffuse mesangial sclerosis (DMS),<sup>16</sup> we included 38 children with DMS (5 familial, 33 sporadic). None of the patients carried mutations in *NPHS1*, *NPHS2* or *WT1*.

DNA samples from 484 healthy Caucasian persons (382 Italian and 102 Turkish) were used as controls.

The study was approved by the Ethics Committee of the Azienda Sanitaria Locale, Bergamo, Italy. Participants or their parents or guardians gave written informed consent.

### Study Assessments and Methods

Methods are described in detail in the Supplementary Appendix, Supplementary Fig. 1 and Supplementary Tables 1–2. Briefly, whole-genome linkage analysis was performed in the index family using a 1-million SNP array. A customized sequence capture array was used to isolate genomic DNA of the positive linkage region, which was sequenced on a 454 GS-FLX platform. Myo1E localization in control and patient kidneys, in cultured podocytes and colocalization with other podocyte proteins were assessed by immunofluorescence (IF) and immunoperoxidase staining and by immunogold electron microscopy (EM). Wild-type and mutant recombinant Myo1E proteins were expressed in cultured podocytes and their intracellular localization and effects on cytoskeletal and on other podocyte proteins and on podocyte motility were evaluated. The effect of Myo1E deficiency on podocyte motility was assessed by knocking down *MYO1E* with *siRNA*.

## RESULTS

### Clinical History and Histology of Patients with MYO1E Mutations

**Index Family**—The proband (SN72) presented with nephritic-range proteinuria, microhematuria, hypoalbuminemia and edema at 9 years (Fig. 1A and Table 1). Thirty percent of glomeruli had segmental sclerohyalinosis with capsular crescents and flocculocapsular adhesion, and 30% showed global sclerohyalinosis and collapse. The remaining glomeruli had focal mesangial hyperplasia, as well as tubular atrophy with tubulitis and moderate interstitial inflammatory infiltrate. Diffuse glomerular parietal deposits of IgM, C3, C4 and C1q and peritubular deposits of IgA, IgG and C3 were present. Electron microscopy was not done. The proband was treated with prednisone, cyclosporine A (CsA) and an ACE-inhibitor, without reduction of proteinuria. After one year of therapy, prednisone and CsA were stopped. Renal function progressively deteriorated, and ESKD developed at 13 years. At 17 years she received a cadaveric kidney transplant. One year after transplant, graft function was normal and there was no proteinuria. After FSGS diagnosis in the proband, the other two siblings (SN73 and SN75) were found to have proteinuria and milder renal injury, with 10–30% of glomeruli affected by segmental or diffuse

sclerohyalinosis with segmental flocculocapsular adhesion and mesangial hyperplasia. Parietal and mesangial focal deposition of IgM, C3 and C1q and peritubular staining for IgG, C3 and C4 were observed in their biopsies. The histology of all three siblings are compatible with FSGS NOS.<sup>1</sup> While with the proband did not respond to glucocorticosteroids and CsA, both siblings had a decrease but not disappearance of proteinuria with CsA (Table 1).

**Family IST**—(Fig. 1B). The proband (IST012) presented with edema, nephrotic-range proteinuria (Table 1), hematuria and hypoalbuminemia at a year of age. A kidney biopsy at 4 years showed 20% of glomeruli with segmental or global sclerosis (Supplementary Fig. 2) and focal tubular dilatation and atrophy with interstitial fibrosis. Focal glomerular IgG, IgA and C3 staining was found. These features are all compatible with FSGS NOS. No Myo1E staining was found with two antibodies against the C-terminus of Myo1E (Supplementary Fig. 3). Glomerular synaptopodin staining was greatly reduced, while podocin staining was almost normal (Supplementary Fig. 3). EM examination showed foot-process effacement and podocyte microvillus transformation, focal thickening and disorganization of the GBM and loss of identifiable layers (Fig. 1C and E), and focal mesangial matrix expansion. These changes are almost identical to those of *Myo1e*-deficient mice<sup>19</sup> (Fig. 1D and F and Supplementary Fig. 4). Other abnormalities included multilamination in the basement membrane of the Bowman's capsule, focal mesangial interposition in the GBM and mesangial electron dense areas.

From 1.5 to 13 years of age the patient received glucocorticosteroids alone or in combination with cyclophosphamide or CsA. She reached a nadir of proteinuria with CsA (Supplementary Fig. 5), without achieving complete remission. She is presently on ramipril and losartan, and she has mild edema, proteinuria (Table 1) and microhematuria. Renal function and blood pressure are normal. Her older sister had presented with microhematuria and mild proteinuria at age 3 months. Renal biopsy showed segmental glomerular hyalinization and GBM thickening associated with mesangial proliferation. IF and EM were not done. She received glucocorticosteroids (no CsA nor ACE-inhibitors). Renal function progressively deteriorated to ESKD; she died at 6 years.

No relevant extrarenal manifestations were reported in affected members of either family, excluding syndromic FSGS.

### Genetic and Functional Studies

Whole-genome multipoint linkage analysis of the three siblings and the father of the index family (Fig. 1A) showed a unique positive peak ( $LOD_{max}=1.9$ ,  $Z_{max}=2.7$ , Fig. 2A) on chromosome 15q21. We also genotyped the mother for 9 rare SNPs in the linkage peak, with rs7181069 reaching the highest LOD score of 2.7 ( $Z=7.4$ ), and defined a new putative locus for FSGS. The linkage area spanned 16Mb between rs12900916 and rs2278545. The expected length of the Inherited-By-Descent (IBD) region around the disease locus is a function of the sibling inbreeding (Inbreeding Coefficient  $F=0.00195$ ), predicting a ~16cM IBD region.<sup>20</sup>

The 112 genes in this region were screened by genomic locus capture followed by high-throughput sequencing in the proband. There were 2141 homozygous mismatches, of which 3 were putative functional variants not reported in SNP databases (two splice variants and one non-synonymous change). Only the coding variant was predicted as probably damaging by bioinformatic analysis (Supplementary Table 3). There is a G→C change in exon 6 of *MYO1E* (c.475G>C) replacing alanine-159 of Myo1E by proline (p.A159P). Direct sequencing showed that the three affected siblings were homozygous and the unaffected

parents heterozygous for the mutation, confirming that the mutation segregates with FSGS (Fig. 2B left). The mutation was not found in 764 normal Italian human chromosomes.

Myo1E is a membrane-associated class I myosin with a motor-head domain that binds ATP and F-actin, a calmodulin-binding neck domain and a tail domain (Fig. 2C).<sup>21–23</sup> The amino acid A159 is highly conserved in myosins from protozoa to humans and lies in the Switch-1 loop of the motor-head domain (Fig. 2C–D).<sup>24</sup> Our structural tridimensional model shows that the Switch-1 region is located in the ATP-binding pocket close to the actin-binding domain (Supplementary Fig. 6).

*MYO1E* was sequenced in the other patients, and a homozygous nonsense mutation (c. 2085T>G) was identified in a second family in a girl with familial FSGS (Fig. 1B). This mutation causes protein interruption at tyrosine 695 (p.Y695X), at the start of the calmodulin-binding domain (Fig. 2B–C and Supplementary Fig. 6). Her parents and her unaffected brother were heterozygous for this mutation (Fig. 1B), which was not found in 968 (764 Italian and 204 Turkish) normal human chromosomes.

The other non-disease causing *MYO1E* variants found in patient cohort are shown in Supplementary Table 4.

Myo1e has been localized in podocytes in mice, and *Myo1e*-knockout mice exhibit proteinuria, podocyte injury and chronic renal disease.<sup>19</sup> Immunohistochemistry on control human kidney biopsies demonstrated that Myo1E is predominantly expressed in the glomerulus (Fig. 3A and Supplementary Fig. 7). Myo1E partially co-localized with synaptopodin, a podocyte specific protein essential for the integrity of podocyte cytoskeleton,<sup>25</sup> but not with the endothelial marker VE-cadherin (Fig. 3B–C), indicating that, as in mice, human Myo1E is mainly expressed in podocytes. Myo1E expression in human podocytes was confirmed by Western-blot (Supplementary Fig. 8). In cultured human podocytes Myo1E localized close to the cytoplasmic membrane with enrichment at the lamellipodia tips (Fig. 3D–F). In co-staining experiments Myo1E localized at the tips of F-actin bundles (Fig. 3D–F) and partially co-localized with CD2AP (Fig. 3G). Immunogold labelling for Myo1E of control human glomeruli revealed gold particles almost exclusively on the cytoplasmic side of the podocyte plasma membrane (Fig. 3H–I).

Human podocytes transfected with wild-type or E753K, I531M, D465N and F307L (control SNPs) Myo1E-GFP showed predominant localization at the plasma membrane, whereas podocytes transfected with A159P-mutant Myo1E-GFP showed a diffuse cytoplasmic localization, which at a higher plasmid dose acquired a punctate pattern (Fig. 4 A–F and Supplementary Figs. 9 and 10).

Similar findings were observed in mouse podocytes and HEK293 cells (Supplementary Figs. 11 and 12). Total internal reflection fluorescence microscopy (TIRF) on live mouse podocytes showed wild-type Myo1E-EGFP in a bright discrete punctate pattern on lamellipodia, filopodia and in endocytic invaginations on the bottom surface of plasma membrane (Supplementary Fig. 14 and Supplementary TIRF movie), while the A159P Myo1E-EGFP was mainly cytosolic (Supplementary Fig. 14).

At variance with wild-type Myo1E, the A159P-mutant did not stain with an anti-Myo1E antibody, suggesting conformational changes in the mutant protein (Supplementary Fig. 9). Wild-type Myo1E-GFP substantially co-stained with F-actin at the podocyte plasma membrane, whereas the A159P mutant did not colocalize with F-actin (Fig. 4G–H).

Wild-type Myo1E partially co-localized with CD2AP at cell surface, while A159P-Myo1E/CD2AP co-staining was mainly cytoplasmic, often punctate (Fig. 4I–L).



Wild-type Myo1E overexpression increased human podocyte motility (Fig. 4M). In contrast, A159P-Myo1E had no effect on podocyte motility. Conversely, Myo1E knockdown in human podocytes (Fig. 4M) and Myo1E knockout in mouse podocytes (Krendel, SUNY Syracuse, personal communication) impaired migration.

A159P-Myo1E transfection did not modify actinin- $\alpha$ -4, podocin, or nephrin expression in podocytes (Supplementary Figs. 15 and 16).

## DISCUSSION

This study identifies two mutations in *MYO1E*, which encodes myosin 1E, a class I non-muscle myosin, which lead to autosomal recessive FSGS. Several findings support the causative role of these mutations in FSGS. First, the segregation of the mutations with the disease; second, the absence of the mutations in a large number of controls; third, the mutations occurring in important functional domains; fourth, the specific expression of Myo1E in human kidney and in cultured podocytes; fifth, the finding that the A159P-Myo1E mutation greatly alters Myo1E subcellular localization, its interaction with podocyte cytoskeleton and its capability to promote podocyte migration; and last, the similarity of the ultrastructural glomerular lesions between the Y695X-Myo1E carrier and *Myo1e*-deficient mice.

The discovery of genetic abnormalities in proteins that bind or regulate the podocyte cytoskeleton<sup>13,14,18</sup> in FSGS highlights the central role of actin cytoskeleton in podocyte morphology and function.<sup>26</sup> The podocyte cytoskeleton is connected to the glomerular basement membrane through  $\alpha$ 3 $\beta$ 1 integrins and by a trimolecular non-muscle myosin-actin-utrophin complex attached to  $\alpha$ - and  $\beta$ -dystroglycans.<sup>5,26,27</sup> Foot process effacement, the hallmark of podocyte injury, is often accompanied by the disappearance of these aligned filaments.<sup>28,29</sup> The cytoskeleton filaments of human podocyte foot processes contain non-muscle myosins IIa and IIb.<sup>30</sup> The present study documents that Myo1E is specifically expressed in human podocytes and is associated with the plasma membrane. The observed enrichment of Myo1E in podocyte processes in conjunction with F-actin filament tips, implicates this protein as a key component of foot process cytoskeleton.<sup>27</sup> Myo1E is important for podocyte morphology and spreading on the extracellular matrix as documented by the observation that *Myo1e*-deficient mice have defects in podocyte organization with foot process effacement.<sup>19</sup> The phenotype of *Myo1e*-deficient mice is characterized by proteinuria, hemoglobinuria, glomerulosclerosis and renal function impairment,<sup>19</sup> features also present in patients with *MYO1E* mutations. Glomeruli of both *Myo1e*-deficient mice<sup>19</sup> and the patient with the Y695X mutation exhibit peculiar ultrastructural features with thickening and disorganization of the GBM, implying that Myo1E plays a role in regulating the crosstalk between podocytes and their matrix.

Non-muscle myosin activity generates tension, and the interaction between actin, myosins and  $\alpha$ -actinin-4 likely allows the foot processes to generate the contractile forces that help the glomerular capillaries to resist the high intraluminal hydrostatic pressure and to change their morphology actively, which would modify the permeability of the glomerular filtration barrier.<sup>26,30,31</sup> Mutations in *MYH9*, encoding the non-muscle myosin heavy-chain IIA, cause autosomal-dominant disorders with macrothrombocytopenia, leukocyte inclusions and, variably, glomerulopathy.<sup>32</sup> Multiple *MYH9* SNPs have been associated with idiopathic and HIV-FSGS and with hypertensive ESKD in African-Americans.<sup>33</sup> However, a follow-up study indicated that the strongest association no longer clustered in *MYH9* but in the neighboring *APOL1*.<sup>34</sup>

The A159P missense mutation here identified impairs the capability of Myo1E to promote podocyte motility, consistent with 159P localization within the Switch-1 loop in the motor head of Myo1E. The Switch-1 is highly conserved among myosins and, together with P-loop and Switch-2 form the ATP-binding domain of myosins.<sup>24</sup> Both in human and mouse podocytes the A159P-Myo1E mutant, at variance with wild-type Myo1E, was mislocalized to the cytoplasm, indicating an important role of the Switch-1 loop for proper subcellular distribution of Myo1E. Mutations in the Switch-1 of another non-muscle myosin (*MYO7A*) cause the Usher type 1b syndrome (deafness and retinitis pigmentosa),<sup>35</sup> confirming the important role of Switch-1 for non-muscle myosin function.

The second mutation causes the formation of a truncated protein that lacks the calmodulin domain, important for calcium-mediated regulation of actin-binding and ATP-hydrolysis,<sup>36</sup> and the tail domain, and likely results in a non-functional protein, mimicking the condition of *Myo1e*-deficient mice. Indeed, the glomerular ultrastructural lesions in the patient and in *Myo1e*-deficient mice were quite similar.

While Myo1E is expressed in several tissues, neither patients with *MYO1E* mutations nor *Myo1e*-deficient mice had any extrarenal involvement, indicating that Myo1E is dispensable for the normal physiology and function of extrarenal tissues and organs.

While patients with *MYO1E* mutations and FSGS were glucocorticosteroid-resistant, three of them had a partial response to CsA therapy. CsA reduces proteinuria in up to 70% of glucocorticosteroid-resistant FSGS patients, although relapse occurs in 40–60%.<sup>37,38</sup> Recently the anti-proteinuric effect of CsA in glucocorticosteroid-resistant FSGS has been attributed to its direct stabilizing effects on the podocyte cytoskeleton rather than to its immunosuppressive actions.<sup>39,40</sup> Whether such mechanisms may have limited the deleterious consequences of *MYO1E* mutations remains to be clarified.

Of note, one affected member in each family developed ESKD whereas the others had milder courses, possibly attributable to earlier diagnosis (Index family) or to effective anti-proteinuric treatment (IST family).

FSGS is genetically heterogeneous, with mutations in several genes,<sup>11–18</sup> each accounting for small percentages of patients. *MYO1E* mutations do not appear to be a common cause of FSGS, as we have found only two independent *MYO1E* mutations among 29 unrelated patients with familial FSGS and none in sporadic cases. Both mutations were homozygous, suggesting that Myo1E-associated FSGS might be restricted to families with some degree of consanguinity.

In conclusion, these studies demonstrate a role of *MYO1E* mutations in FSGS and suggest the importance of Myo1E in podocyte homeostasis and the consequent integrity of the glomerular permselective barrier.

## Supplementary Material

Refer to Web version on PubMed Central for supplementary material.

## Acknowledgments

This study has been partially supported by a grant from the E-Rare program (PodoNet), from Fondazione “La Nuova Speranza” Onlus, Milan, Italy, from Fondazione ARMIR Onlus Aiuti per la Ricerca sulle Malattie Rare (Bergamo, Italy), from Fondazione ART Onlus per la Ricerca sui Trapianti Milan, Italy and from the NephCure Foundation.

F. Hildebrandt is an investigator of the Howard Hughes Medical Institute, the Frederick G. L. Huetwell professor, and a Doris Duke Distinguished Clinical Scientist, and is supported by grants from the National Institutes of Health (NIH; R01-DK076683 and RC1-DK086542). R. Piras and C. Mele are recipients of fellowships from Fondazione ART. F. Ozaltin is supported by a grant from The Scientific and Research Council of Turkey (TUBITAK, grant number 108S417).

The Authors wish to greatly thank Professor Giuseppe Ippolito, who was instrumental for establishing the collaboration between the L. Spallanzani Institute and the Mario Negri Institute for the next generation sequencing; Dr Luisa Murer and Professor Paola Romagnani for recruiting patients, Dr Alberto Ferrarini for the support in Nimblegen genomic enrichment, Dr Elena Bresin for support of the Italian Registry of FSGS, Dr Samantha Solini for immunostaining in control kidney biopsies, Dr Elena Gagliardini and Daniela Rottoli for immunogold electron microscopy, and Professor Daniele Cusi for discussion of linkage results. Laura Bottanelli, Sergio Carminati, Davide Martinetti and Simone Manini provided informatic support. The Authors are deeply indebted with Dr Mauro Abbate for critical examination of patients' biopsies and for help in the selection of light microscopy and electron microscopy images. The Authors also thank Howard Wynder at Histology and Microscopy Core, Washington University in St. Louis, for processing mouse kidney samples for EM and Sharon Chase, Anna Pezzotta and Chris Pellenz for excellent technical help. Conditionally immortalized human and mouse podocytes were generous gifts of Dr. M. Saleem (University of Bristol, UK) and Dr. P. Mundel (Massachusetts General Hospital, MA), respectively.

## References

1. D'Agati VD, Fogo AB, Bruijn JA, Jennette JC. Pathologic classification of focal segmental glomerulosclerosis: a working proposal. *Am J Kidney Dis.* 2004; 43:368–382. [PubMed: 14750104]
2. Barisoni L, Schnaper HW, Kopp JB. A proposed taxonomy for the podocytopathies: a reassessment of the primary nephrotic diseases. *Clin J Am Soc Nephrol.* 2007; 2:529–542. [PubMed: 17699461]
3. Pollak MR. Focal segmental glomerulosclerosis: recent advances. *Curr Opin Nephrol Hypertens.* 2008; 17:138–142. [PubMed: 18277145]
4. Löwik MM, Groenen PJ, Levchenko EN, Monnens LA, van den Heuvel LP. Molecular genetic analysis of podocyte genes in focal segmental glomerulosclerosis--a review. *Eur J Pediatr.* 2009; 168:1291–1304. [PubMed: 19562370]
5. Chiang CK, Inagi R. Glomerular diseases: genetic causes and future therapeutics. *Nat Rev Nephrol.* 2010; 6:539–554. [PubMed: 20644582]
6. Machuca E, Benoit G, Antignac C. Genetics of nephrotic syndrome: connecting molecular genetics to podocyte physiology. *Hum Mol Genet.* 2009; 18:R185–R194. [PubMed: 19808795]
7. Filler G, Young E, Geier P, Carpenter B, Drukker A, Feber J. Is there really an increase in non-minimal change nephrotic syndrome in children? *Am J Kidney Dis.* 2003; 42:1107–1113. [PubMed: 14655180]
8. Braden GL, Mulhern JG, O'Shea MH, Nash SV, Ucci AA Jr, Germain MJ. Changing incidence of glomerular diseases in adults. *Am J Kidney Dis.* 2000; 35:878–883. [PubMed: 10793022]
9. Kitiyakara C, Eggers P, Kopp JB. Twenty-one-year trend in ESRD due to focal segmental glomerulosclerosis in the United States. *Am J Kidney Dis.* 2004; 44:815–825. [PubMed: 15492947]
10. Haas M, Spargo BH, Coventry S. Increasing incidence of focal-segmental glomerulosclerosis among adult nephropathies: a 20-year renal biopsy study. *Am J Kidney Dis.* 1995; 26:740–750. [PubMed: 7485126]
11. Kestila M, Lenkkeri U, Mannikko M, et al. Positionally cloned gene for a novel glomerular protein--nephrin--is mutated in congenital nephrotic syndrome. *Mol Cell.* 1998; 1:575–582. [PubMed: 9660941]
12. Boute N, Gribouval O, Roselli S, et al. NPHS2, encoding the glomerular protein podocin, is mutated in autosomal recessive steroid-resistant nephrotic syndrome. *Nat Genet.* 2000; 24:349–354. [PubMed: 10742096]
13. Kaplan JM, Kim SH, North KN, et al. Mutations in ACTN4, encoding alpha-actinin-4, cause familial focal segmental glomerulosclerosis. *Nat Genet.* 2000; 24:251–256. [PubMed: 10700177]
14. Kim JM, Wu H, Green G, et al. CD2-associated protein haploinsufficiency is linked to glomerular disease susceptibility. *Science.* 2003; 300:1298–1300. [PubMed: 12764198]
15. Winn MP, Conlon PJ, Lynn KL, et al. A mutation in the TRPC6 cation channel causes familial focal segmental glomerulosclerosis. *Science.* 2005; 308:1801–1804. [PubMed: 15879175]



16. Hinkes B, Wiggins RC, Gbadegesin R, et al. Positional cloning uncovers mutations in PLCE1 responsible for a nephrotic syndrome variant that may be reversible. *Nat Genet.* 2006; 38:1397–1405. [PubMed: 17086182]
17. Mucha B, Ozaltin F, Hinkes BG, et al. Mutations in the Wilms' tumor 1 gene cause isolated steroid resistant nephrotic syndrome and occur in exons 8 and 9. *Pediatr Res.* 2006; 59:325–331. [PubMed: 16439601]
18. Brown EJ, Schlondorff JS, Becker DJ, et al. Mutations in the formin gene INF2 cause focal segmental glomerulosclerosis. *Nat Genet.* 2009; 42:72–76. [PubMed: 20023659]
19. Krendel M, Kim SV, Willinger T, et al. Disruption of Myosin 1e promotes podocyte injury. *J Am Soc Nephrol.* 2009; 20:86–94. [PubMed: 19005011]
20. Genin E, Todorov AA, Clerget-Darpoux F. Optimization of genome search strategies for homozygosity mapping: influence of marker spacing on power and threshold criteria for identification of candidate regions. *Ann Hum Genet.* 1998; 62:419–429. [PubMed: 10088039]
21. El Mezgueldi M, Tang N, Rosenfeld SS, Ostap EM. The kinetic mechanism of Myo1e (human myosin-1C). *J Biol Chem.* 2002; 277:21514–21521. [PubMed: 11940582]
22. Yu HY, Bement WM. Multiple myosins are required to coordinate actin assembly with coat compression during compensatory endocytosis. *Mol Biol Cell.* 2007; 18:4096–4105. [PubMed: 17699600]
23. Krendel M, Osterweil EK, Mooseker MS. Myosin 1E interacts with synaptojanin-1 and dynamin and is involved in endocytosis. *FEBS Lett.* 2007; 581:644–650. [PubMed: 17257598]
24. Forgacs E, Sakamoto T, Cartwright S, et al. Switch 1 mutation S217A converts myosin V into a low duty ratio motor. *J Biol Chem.* 2009; 284:2138–2149. [PubMed: 19008235]
25. Asanuma K, Yanagida-Asanuma E, Faul C, Tomino Y, Kim K, Mundel P. Synaptopodin orchestrates actin organization and cell motility via regulation of RhoA signalling. *Nat Cell Biol.* 2006; 8:485–491. [PubMed: 16622418]
26. Faul C, Asanuma K, Yanagida-Asanuma E, Kim K, Mundel P. Actin up: regulation of podocyte structure and function by components of the actin cytoskeleton. *Trends Cell Biol.* 2007; 17:428–437. [PubMed: 17804239]
27. Nabet B, Tsai A, Tobias JW, Carstens RP. Identification of a putative network of actin-associated cytoskeletal proteins in glomerular podocytes defined by co-purified mRNAs. *PLoS One.* 2009; 4:e6491. [PubMed: 19652713]
28. Kerjaschki D. Caught flat-footed: podocyte damage and the molecular bases of focal glomerulosclerosis. *J Clin Invest.* 2001; 108:1583–1587. [PubMed: 11733553]
29. Takeda T, McQuistan T, Orlando RA, Farquhar MG. Loss of glomerular foot processes is associated with uncoupling of podocalyxin from the actin cytoskeleton. *J Clin Invest.* 2001; 108:289–301. [PubMed: 11457882]
30. Drenckhahn D, Franke RP. Ultrastructural organization of contractile and cytoskeletal proteins in glomerular podocytes of chicken, rat, and man. *Lab Invest.* 1988; 59:673–682. [PubMed: 3141719]
31. Friedrich C, Endlich N, Kriz W, Endlich K. Podocytes are sensitive to fluid shear stress in vitro. *Am J Physiol Renal Physiol.* 2006; 291:F856–F865. [PubMed: 16684926]
32. Singh N, Nainani N, Arora P, Venuto RC. CKD in MYH9-related disorders. *Am J Kidney Dis.* 2009; 54:732–740. [PubMed: 19726116]
33. Kopp JB, Smith MW, Nelson GW, et al. MYH9 is a major-effect risk gene for focal segmental glomerulosclerosis. *Nat Genet.* 2008; 40:1175–1184. [PubMed: 18794856]
34. Genovese G, Tonna SJ, Knob AU, et al. A risk allele for focal segmental glomerulosclerosis in African Americans is located within a region containing APOL1 and MYH9. *Kidney Int.* 2010
35. Roux AF, Faugere V, Le Guedard S, et al. Survey of the frequency of USH1 gene mutations in a cohort of Usher patients shows the importance of cadherin 23 and protocadherin 15 genes and establishes a detection rate of above 90%. *J Med Genet.* 2006; 43:763–768. [PubMed: 16679490]
36. Adamek N, Coluccio LM, Geeves MA. Calcium sensitivity of the cross-bridge cycle of Myo1c, the adaptation motor in the inner ear. *Proc Natl Acad Sci U S A.* 2008; 105:5710–5715. [PubMed: 18391215]

37. Cattran DC, Appel GB, Hebert LA, et al. A randomized trial of cyclosporine in patients with steroid-resistant focal segmental glomerulosclerosis. North America Nephrotic Syndrome Study Group. *Kidney Int.* 1999; 56:2220–2226. [PubMed: 10594798]
38. Meyrier AY. Treatment of focal segmental glomerulosclerosis with immunophilin modulation: when did we stop thinking about pathogenesis? *Kidney Int.* 2009; 76:487–491. [PubMed: 19494796]
39. Faul C, Donnelly M, Merscher-Gomez S, et al. The actin cytoskeleton of kidney podocytes is a direct target of the antiproteinuric effect of cyclosporine A. *Nat Med.* 2008; 14:931–938. [PubMed: 18724379]
40. Mathieson PW. Proteinuria and immunity--an overstated relationship? *N Engl J Med.* 2008; 359:2492–2494. [PubMed: 19052132]

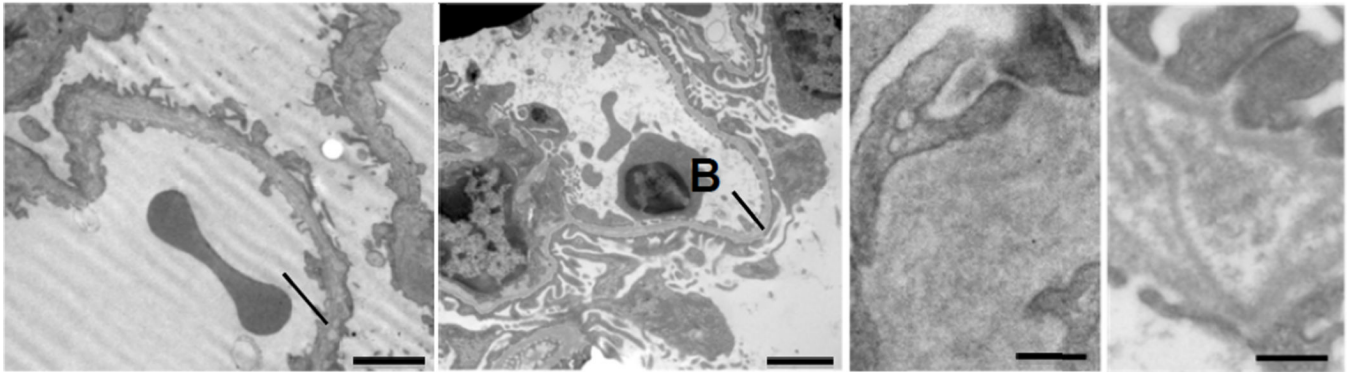
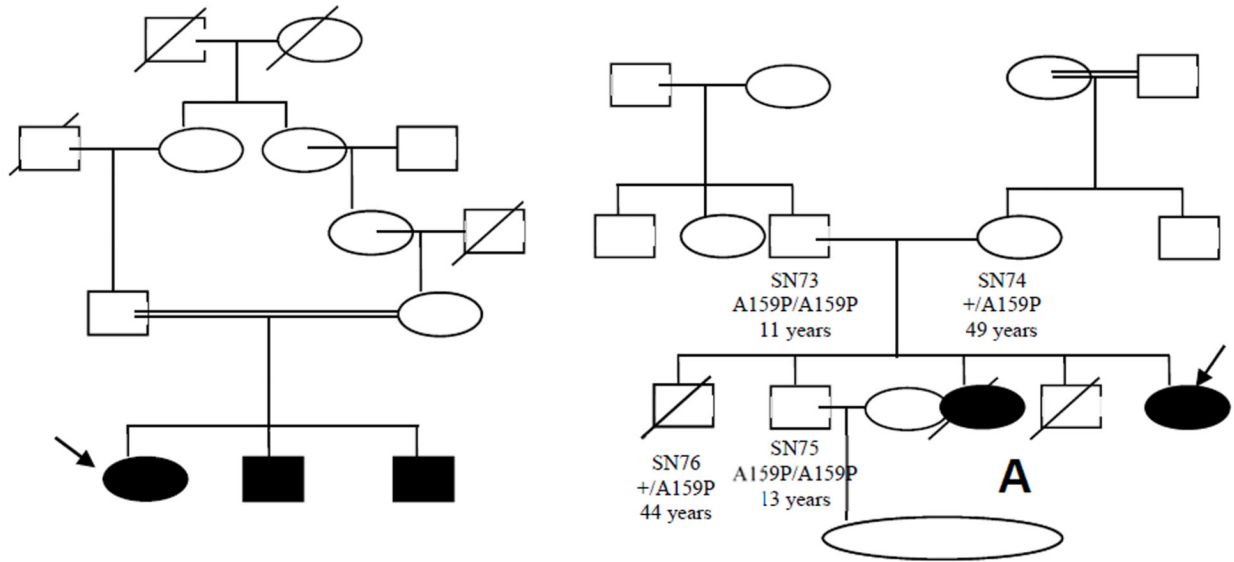
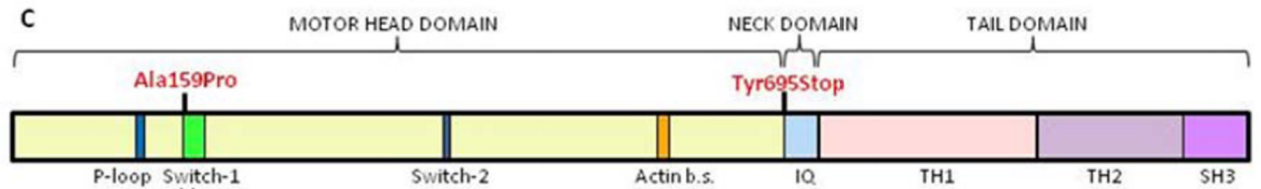
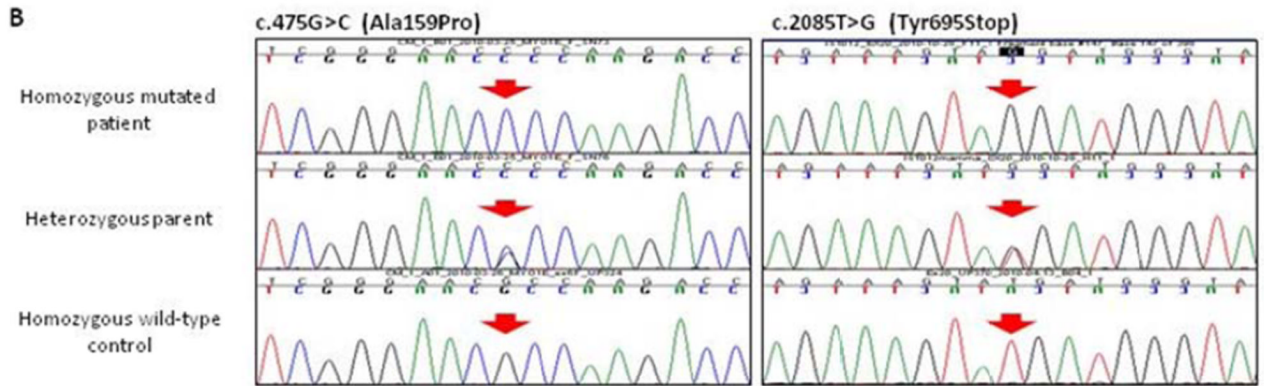
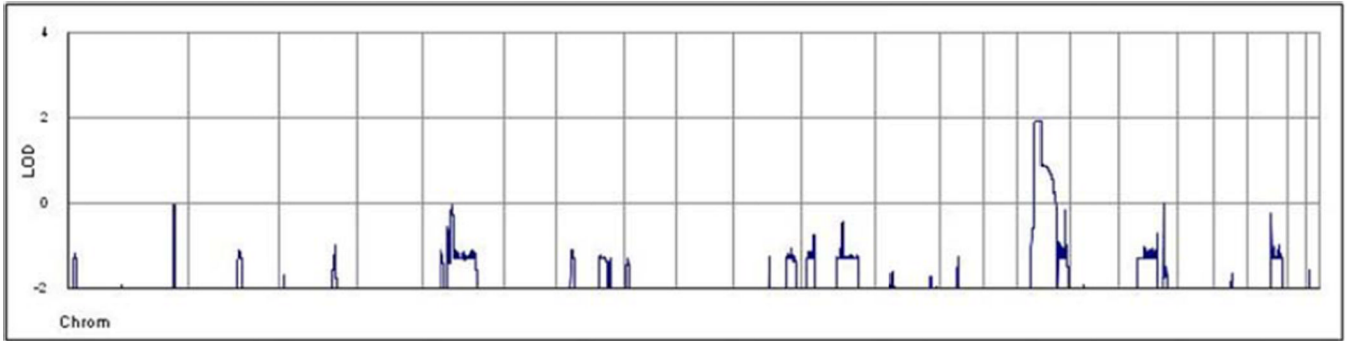


**Figure 1.**

**Panels A–B.** Pedigrees of the families with *MYO1E* mutations. Panel A shows the pedigree of the index family and Panel B, the IST family. The probands are indicated with an arrow, plus indicates the wild-type allele; A159P and Y695X indicate the c.475G>C and the c.2085T>G mutations, in the transcript of *MYO1E*, corresponding to the amino acid changes Ala159Pro and Tyr695Stop, respectively. Squares indicate male family members, and circles, female; slashes indicate deceased persons. Solid symbols: persons with FSGS. The double horizontal bars indicate consanguinity. The parents of IST012 are from the same village. IST012 was homozygous in all SNPs in *MYO1E* (Supplementary Table 5) indicating consanguinity. Identification codes and ages at last observation (or at death) are shown when available. na: DNA not available. \*Died at 13 years of age due to meningitides; °perinatal sudden death. **Panels C–F.** Ultrastructural changes of the glomerular capillary wall in patient IST012 with the homozygous Y695X Myo1E mutation (C and E) and in *myo1e*-knockout mice (D: 2 months, F: 4 months old). Both in the patient and in mice, the glomerular basement membrane (BM) is thickened and disorganized with multiple electron lucent areas and multilamination. Intramembranous granular material is seen in lucent areas between laminae. Foot processes are effaced. Intercellular contacts focally show increased density of plasma membranes (panel E). Podocytes show microvillous transformation (original magnification, C and D,  $\times 12,000$ , scale bars are shown).



**D**

Mutation	Sequence
Homo sapiens	...GGG <b>T</b> KVQHVKDI ILQSNPLLEAFGNA <b>K</b> TVRNNNSSRFGRYFEIQFSPGGE <b>P</b> ...
Pan troglodytes	...GGG <b>T</b> KVQHVKDI ILQSNPLLEAFGNA <b>K</b> TVRNNNSSRFGRYFEIQFSPGGE <b>P</b> ...
Macaca mulatta	...GGG <b>P</b> KVQHVKDI ILQSNPLLEAFGNA <b>K</b> TVRNNNSSRFGRYFEIQFSPGGE <b>P</b> ...
Mus musculus	...GGG <b>P</b> KVQHVKDI ILQSNPLLEAFGNA <b>K</b> TVRNNNSSRFGRYFEIQFSPGGE <b>P</b> ...
Rattus norvegicus	...GGG <b>P</b> KVQHVKDI ILQSNPLLEAFGNA <b>K</b> TVRNNNSSRFGRYFEIQFSPGGE <b>P</b> ...
Canis familiaris	...GGG <b>P</b> KVQHVKDI ILQSNPLLEAFGNA <b>K</b> TVRNNNSSRFGRYFEIQFSPGGE <b>P</b> ...
Equus caballus	...GGG <b>P</b> KVQHVKDI ILQSNPLLEAFGNA <b>K</b> TVRNNNSSRFGRYFEIQFSPGGE <b>P</b> ...
Gallus gallus	...GGG <b>P</b> KVQHVKDI ILQSNPLLEAFGNA <b>K</b> TVRNNNSSRFGRYFEIQFSPGGE <b>P</b> ...
Xenopus laevis	...GGG <b>P</b> KVQHVKDI ILQSNPLLEAFGNA <b>K</b> TVRNNNSSRFGRYFEIQFSPGGE <b>P</b> ...
Danio rerio	...GGG <b>P</b> RVQHVKDI ILQSNPLLEAFGNA <b>K</b> TVRNNNSSRFGRYFEIQFSSGGE <b>P</b> ...
Dictyostelium discoideum	...SNQSN <b>G</b> ERTISKMLLD <b>S</b> NPLLEAFGNA <b>K</b> TLRNDNSSRFGRYMEMQFN <b>V</b> AVG <b>S</b> P...

**Figure 2. Identification of MYO1E mutations in FSGS**

**Panel A.** Parametric multipoint LOD score profile across the human genome, calculated in the index family. Note the single peak of positivity on human chromosome 15. **Panel B (Left).** Sequence electropherograms of the index family. The affected child has a homozygous G>C substitution (arrow), while the unaffected father is heterozygous for the mutation. **Panel B (Right).** Sequence electropherograms of the IST family. The affected child has a homozygous T>G substitution (arrow), while the unaffected mother is heterozygous for the mutation. The bottom electropherograms are from healthy controls. **Panel C.** Functional domains in myosin 1E (Myo1E) protein. Myo1E contains a motor head domain (that includes a P-loop, a Switch-1 and a Switch-2 domains) that binds ATP and F-

actin (Actin b.s.), a light-chain binding neck domain (IQ) that binds calmodulin and a tail, containing lipid binding tail homology-1 (TH1), proline-rich tail homology-2 (TH2) and Src homology-3 (SH3) domains. The Ala159Pro change is within the Switch-1 region. The Y695X causes a truncation at the beginning of the neck domain. **Panel D.** Sequence alignment of the Myo1E protein and homologues among various species. The red frame indicates the location of the highly conserved Ala159 amino acid that in the index family is changed to Pro (P). Sequences were from the National Center for Biotechnology Information.



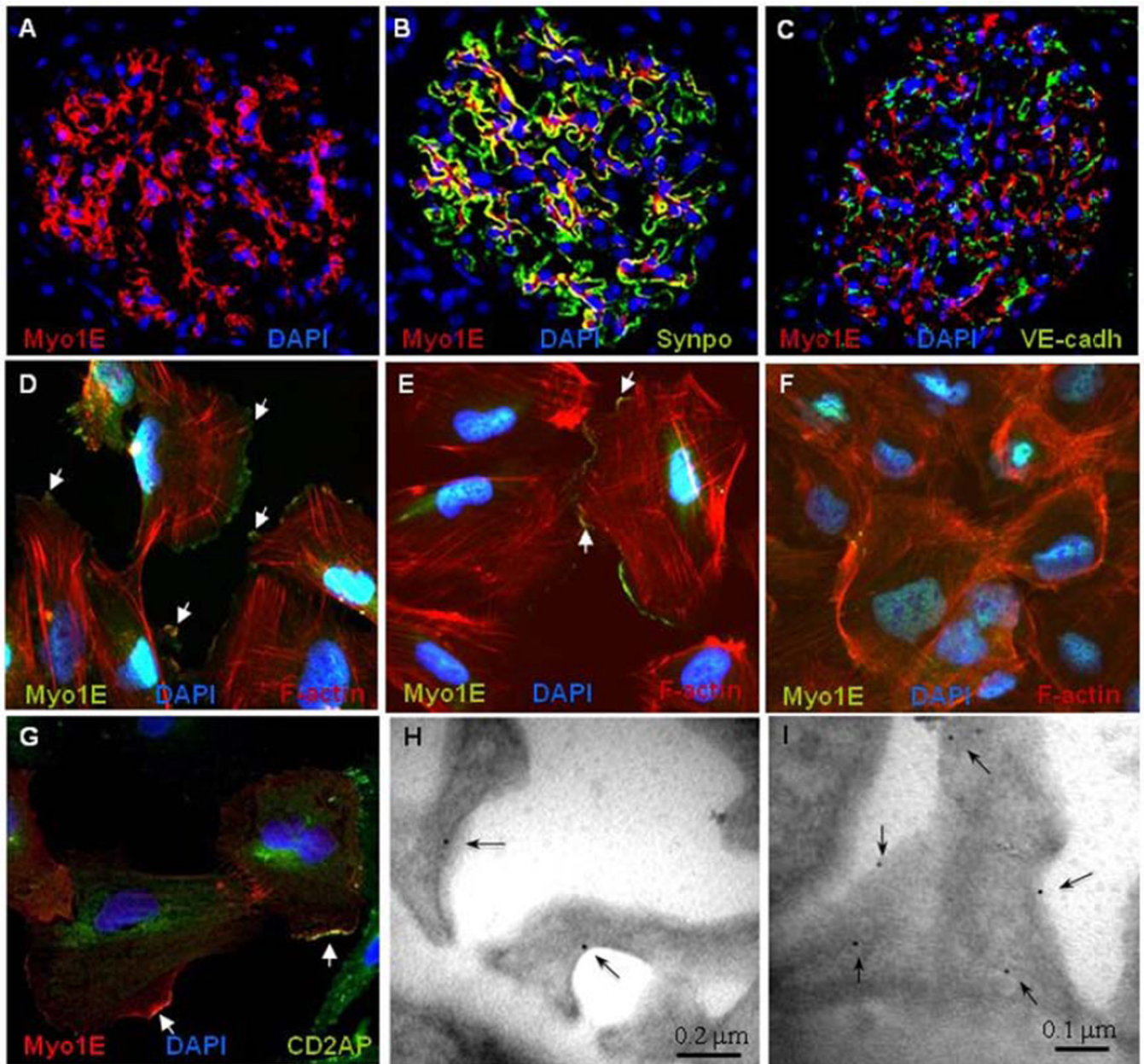


### Figure 3. Endogenous Myo1E Expression

**Panels A–C.** Immunofluorescence staining of normal human kidney with DAPI (blue) for cell nuclei and antibodies against myosin 1E (Myo1E, red, panel A) and the podocyte marker synaptopodin (Synpo, green, panel B) or the endothelial cell marker VE-cadherin (VE-Cadh, green, panel C). Myo1E staining is observed in the glomerulus. The yellow color shows the merge of the Myo1E and the synaptopodin stainings in the podocytes. **Panels D–F.** Staining of endogenous Myo1E in cultured undifferentiated (panel D), terminally differentiated non confluent (14 day culture at 37 °C, panel E) and confluent human podocytes (panel F). The Myo1E staining (green) shows predominant localization along the plasma membrane, mainly on cell lamellipodia both in undifferentiated and in fully differentiated podocytes and fainter staining in confluent podocytes. The white arrows show areas of colocalization between Myo1E and the F-actin tips (stained by rhodamine-

phalloidin, red) (merge yellow). **Panel G.** Partial co-staining (yellow, white arrows) of endogenous Myo1E (red) and CD2AP (green) in cultured differentiated podocytes. Original magnification 400 $\times$ .

**Panels H–I.** Representative pattern of immunogold labelling for Myo1E in podocytes of control human glomeruli. Gold particles (arrows) are localized on the cytoplasmic side of the podocyte plasma membrane. Original magnification,  $\times 44,000$  (scale bars are shown).

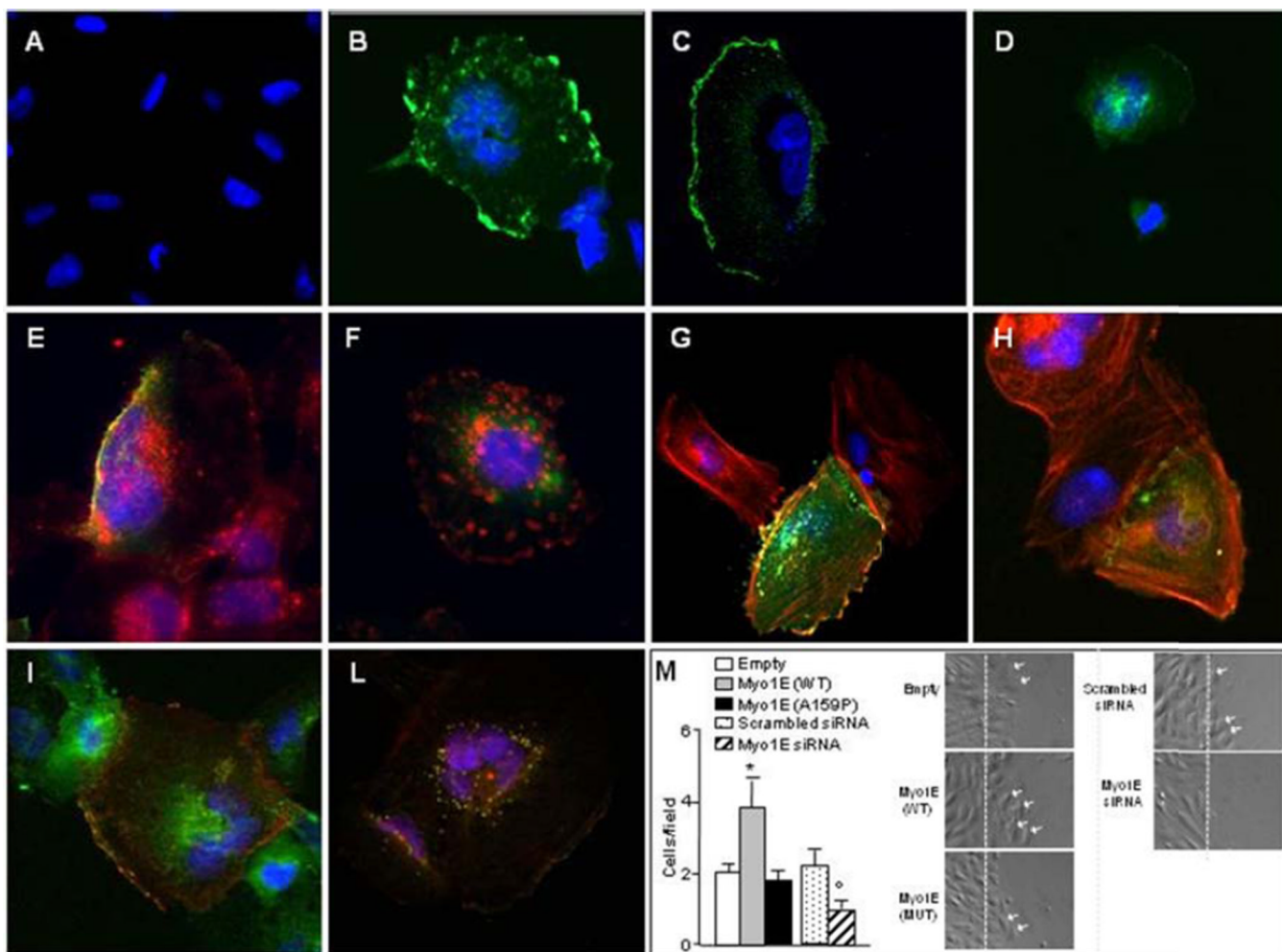


#### Figure 4. Expression of recombinant Myo1E in cultured podocytes

**Panels A–D.** Undifferentiated human podocytes transfected with wild-type, E753K (control SNP, rs8024923) or mutant A159P GFP-tagged Myo1E (green, 1  $\mu$ g plasmid) and analyzed by confocal microscopy, the nuclei were stained with DAPI (blue). **Panel A.** Untransfected human podocytes. **Panels B–D.** Human podocytes transfected with wild-type Myo1E (panel B), control E753K Myo1E (panel C), or mutant A159P Myo1E (panel D). Wild-type and control E753K Myo1E localize along the plasma membrane while the A159P mutant shows a cytoplasmic distribution. Transfection efficiency was about 30% for the wild-type, E753K and A159P-GFP-tagged constructs (by calculating the ratio between the numbers of green cells and of blue nuclei  $\times 100$  in 10–15 high power fields). **Panels E–F.** Staining of podocyte plasma membranes with rhodamine-labeled lectin (red). Wild-type Myo1E-GFP (panel E) partially colocalizes with lectin (yellow) while the A159P mutant does not (panel F, green). The mislocalization of the mutant protein is not attributable to instability or degradation as the sizes and the amounts of the wild-type and A159P-tagged proteins expressed in transfected podocytes were the same in Western blot (Supplementary Fig. 13A–B). **Panels G–H.** Staining of F-actin filaments (red) in transfected human podocytes. Wild-type Myo1E-GFP (panel G) partially colocalizes with F-actin (yellow) while the A159P mutant does not (panel H, green). **Panels I–L,** staining with an anti-CD2AP antibody (green). Wild-type Myo1E-MYC (panel I, red) partially colocalizes with CD2AP at the plasma membrane

(yellow) while in cells transfected with the A159P mutant (panel L), Myo1E-MYC and CD2AP abnormally co-localize in the cytoplasm (yellow). Original magnification, 400 $\times$ .

**Panel M.** Scrape-wound migration assay of cultured human podocytes. Transfection with wild-type Myo1E-GFP (WT) increases podocyte migration vs. podocytes transfected with empty-GFP (Empty), while the A159P Myo1E-GFP (A159P) has no effect on migration. Knockdown of endogenous Myo1E by siRNA (Myo1E siRNA) reduced podocyte migration vs. podocytes transfected with universal scrambled siRNA (Scrambled siRNA). The numbers of podocytes that migrated into the wound track, 6 h after the podocyte layer was scraped, are shown (podocyte/field, one field=71500  $\mu\text{m}^2$ ). Results are mean  $\pm$ SE of 3 wells (n=5 fields counted/well). Images of representative fields are shown (the dashed lines indicate the left margin of the scrape-wound, the white arrows highlight migrating cells). \*P<0.05 wild-type vs. empty-GFP and A159P (by one-way analysis of variance), °P<0.05 vs Scrambled siRNA (Student's *t*-test).

**Table 1**

Clinical Data on the Patients with *MYO1E* Mutations

Patient ID	Age at diagnosis (years)	Age at ESKD (years)	Treatment	Renal biopsy	Data at first observation			Data at last observation		
					Age years	U-prot g/24h	S-creat mg/dl (μmol/L)	Age years	U-prot g/24h	S-creat mg/dl (μmol/L)
SN72	9	13	Steroids: NR Csa: NR ACEi	Advanced FSGS	9	3.00	0.6 (45.8)	18	0.05 <sup>#</sup>	1.1 <sup>#</sup> (83.9)
SN75	4	-	Csa: PRem ACEi	FSGS	4	1.56	0.4 (30.5)	13	0.53	0.7 (53.4)
SN73	2	-	Steroids: NR Csa: PRem ACEi	FSGS	2	3.40	0.4 (30.5)	11	0.59	0.67 (51.1)
IST012	1	-	Steroids: NR CsA: PRem ACEi	FSGS	1	+++ <sup>o</sup>	0.3 (22.9)	14.5	2.8	0.31 (23.6)

ESKD, end stage kidney disease; U-prot, proteinuria; S-creat, serum creatinine; NR, No response; PRem: Partial Remission; ACEi, ACE-inhibitor.

<sup>o</sup> Evaluated by dipstick. Data in SI are in brackets.

<sup>#</sup> Data observed after kidney transplantation.

Note that the deceased elder sister of IST012 is not included in this table, as she died prior to these studies; no DNA was available.